Low velocity impact response and damage of laminate composite glass fibre/epoxy based tri-block copolymer

R. Matadi Boumbimba [a, c, *], C. Froustey [b], P. Viot [c], P. Gerard [d]

[a] National Engineering School of Metz, Laboratory of Mechanics, Biomechanics, Polymers and Structures, 1 Route d'Ars Laquenexy cs6582, 57078 Metz Cedex 3, France
[b] Université de Bordeaux I2M, UMR CNRS 5295, F-33405 Talence, France
[c] Arts et Métiers Paristech, I2M, UMR CNRS 5295, F-33405 Talence, France
[d] ARKEMA, Groupement de Recherche de Lacq, F-64170 Lacq, France

ABSTRACT

Two types of laminate composites made of glass fibre/epoxy matrix (EPO_FV) and glass fibre/epoxy modified tri-block copolymer (Nanostrength) matrix (EPONS_FV) were manufactured by compression moulding. Some AFM investigations have been done to identify the Nanostrength dispersion in the epoxy matrix and some DMA analyses have been performed, at different frequencies, to understand the frequency or the strain rate sensitivity of both composites. Compared to EPO_FV, EPONS_FV exhibits a significant frequency/strain rate sensitivity. Impact resistance of the composite was investigated by means of low velocity impact tests. The low velocity impact results indicate that the addition of Nanostrength leads to the improved impact resistance and an increase in absorbed energy, especially at high impact energy level. SEM observations, performed on ion polished samples, reveal the presence of micro-cracks for both composites. Micro-cracks consist of a coalescence of fibre matrix de-bonding. It was also observed that EPONS_FV contains a lower density of micro-cracks compared to EPO_FV, confirming the fact that the composite with Nanostrength absorbs more energy by Nanostrength micelles cavitation.

1. Introduction

Due to their poor resistance to damage during low velocity impact events, the use of laminate composites is limited in many industrial applications. The defects created by low-velocity impact events are sometimes not visible to the eye [1,2]. These defects may therefore lead to the sudden collapse of the structure. Low velocity impact is the source of different types of damages such as delamination [3,4] matrix cracking [5], fibre/matrix interfacial debonding and fibre breakage. Among these defects, delamination that is initiated by the extension and the bridging of matrix cracks is the major failure mode during low-velocity impact [4,6–11]. In laminate composites based on epoxy matrix, delamination is strongly related to the brittle nature of epoxy matrix. In this case enhancing the matrix toughness may leads to the improvement of the impact resistance of laminate composites. Previous work has focused on enhancing impact resistance of composites by using epoxy-based nanocomposites as a matrix. Nano-scale reinforcements in composite laminates offer the opportunity to enrich the fibre-matrix interface and enhance the matrix toughening properties, with minimal weight penalty [12]. Due to their small size, rigid nano-fillers have proven to be effective in simultaneously improving the toughness and the stiffness of composites [13–18]. In particular, the well-dispersed silica nanoparticles have been adopted to strengthen epoxy resins [19,20]. Gojny et al. [21] have investigated the tensile properties of glass fibre reinforced carbon nanotube/epoxy matrix. These authors showed that tensile properties of laminates are not affected by the presence of CNTs, while inter-laminar shear strength and fracture toughness are increased.

Other literature dealing with the low velocity impact behaviour of fibres/nanoparticles-epoxy show the advantage of using nano-particle in fibre/composite materials. Hosur et al. [22] showed that the addition of nanoclay in the system reduced the impact damage, though the impact response in terms of peak load remained mostly unaltered. Similar improvements in inter-laminar fracture toughness have been reported. Studies performed by Ávila et al. [23]

showed that the nanoclay presence in glass fibre/epoxy composites led to a more intense formation of delaminated areas after a low velocity impact test. This phenomenon can be attributed to interlaminar shear forces caused by the intercalated nano-structures. The incorporation of nanoclay led to an increase in the energy absorption capacity of glass fibre composites by about 48% when loading with a low energy (20J) was applied. Other studies reported that the use of epoxy-based nanoclay as a matrix leads to the significant improvements of low velocity impact performance of carbon fibre/epoxy laminate composites [24]. In the work of Iqdal et al. [24] the authors observed that for nanoclay content in the matrix up to 3 wt%, both damage resistance and damage tolerance of laminates were improved in terms of both threshold impact energy and incipient impact energy. In the same way, Reis et al. [25,26] have observed that the nanoclay addition increases the maximum load and damaged area. These authors worked on low velocity impact of Kevlar/epoxy based nanoclay. The authors concluded that the increase of impact properties is due to the fact that clays increase the damage area and energy absorption by matrix microcracking.

Based on the method of nanostructuration of the epoxy matrix, the very recent use of acrylic block copolymers, is a very promising methodology. Acrylic block-copolymers have the ability to self-assemble to form nanostructures (e.g. micelles, vesicles) through selective chemical interactions with the epoxy matrix [27]. Being a relatively new method, the use of epoxy modified acrylic block-copolymers as a matrix in laminate composite materials has received less attention. Bashar et al. [28] showed that the fracture behaviour of an epoxy resin can be significantly affected by the presence of nanostructured acrylic tri-block copolymer. These authors demonstrated that the formation of micelle structures by acrylic tri-block-copolymer addition in epoxy led to cavitation during plane-strain fracture, followed by subsequent matrix deformation. These effects were attributed to excellent toughness improvements in the bulk epoxy system. In the work performed by Denneulin et al. [29], which is focused on the study of low velocity impact behaviour of Aramid fibres/epoxy-Acrylate tri-blocks composite laminates, the authors showed that the impact resistance was enhanced in the presence of Acrylic tri-block copolymer(Nanostrength). However, the low velocity impact of epoxy fibre laminate composites also depends on the nature of the fibres. The aramid fibres are known to have high toughness properties, which when combined with their failure mechanisms and damage tolerance, could promote good impact resistance in nano-reinforced epoxy laminate composites. In order to study the effect of these acrylic tri-bloc copolymers in the presence of more rigid fibres, we previously performed work on glass fibre/epoxy resin filled with acrylic tri-bloc copolymers [30]. In this previous study we focussed on the processing, the microstructure characterisation and the thermomechanical properties of laminate composites made of glass fibre/epoxy resin filled with acrylic tri-bloc copolymers (Nanostrength) [30]. Unlike Aramid fibres, the use of Nanostrengh to enhance the impact resistance of glass fibre epoxy composite materials could lead to effective and less expensive applications in manufacturing helmets, boat hulls and aerospace structures.

To that end, the present study aims to investigate the effect of nanostructured tri-block acrylic copolymers on impact resistance in glass fibres epoxy laminate composites. Attention is focused on low-velocity impact tests carried out with a drop-weight tower. Laminate composites, with or without nanostructured tri-block acrylic copolymers, have been tested at different level of impact energies. Post-mortem damage mechanisms at different scale have been investigated using optical and scanning electronic microscopy (SEM).

2. Materials and procedure

The polymer resin used in this work is a thermoset epoxy precursor DGEBA (EPOLAM2020) with low viscosity, supplied by Axson Technologies. The hardener, also supplied by Axson Technologies, is used in a ratio of 0.345 w/w (corresponding to 34.5 g of hardener for 100 g of resin). The fibre fabric used is a plain bi-directional woven fabric glass fibre (supplied by Composites Distribution) with a thickness of 0.15 mm and surface density of 202 g/m^2. The acrylic tri-block copolymers M52N, named Nanostrength (Fig. 1) and supplied by ARKEMA (GRL, France), are symmetric functionalized MAM copolymers. MAM copolymers have a poly(-butyl acrylate) centre block and two poly (methyl methacrylate) side blocks, designed for epoxy formulations such as DGEBA. Prior to composite panel elaboration, the Nanostrength was solubilised in epoxy resin to ensure effective dispersion. The Nanostrength weight concentration in the epoxy resin is equal to 10%. Because the addition of Nanostrength leads to an increase in resin viscosity, a low viscosity di-functional aliphatic reactive diluent (RD107) based on hexanediol (from Epotec) was added to limit the increase of viscosity. In our previous publication [30], the effect of Nanostrength concentration has been studied. It was established that better impact performances are obtained for a Nanostrength amount of 10 wt%. Above this concentration the significant increase of resin viscosity, despite the use of the reactive diluent makes the glass fabrics impregnation difficult. Our composite panel is composed of five woven glass fabrics. Composite panel preparation was performed via the hand lay-up method. After glass fabrics impregnation, hot press equipment operating under a pressure of 10 bars and a temperature of 90 °C was used to cure glass fibre epoxy with (EPONS_FV) or without (EPO_FV) Nanostrength. The last step is the post-curing in an oven at 80 °C for 2 h. The resulting composite plates have dimensions of 200 × 200 × 1 mm^3. Fibre weight fractions of these composite materials, determined by Thermo-gravimetric Analysis (TGA), is about 70%. Detailed information about the material preparation and the morphology characterization has been reported in a previous publication [30].

Atomic force microscopy (AFM) was performed using a high resolution (VEECO type Dimension 3100) in tapping mode. Samples having previously undergone ion polishing were observed in order to determine the Nanostrength shape and distribution in the laminate composite. Scanning electron microscopy (SEM) (JSM 840) was used to investigate the composite plates after impact testing.

In order to quantify the effect of Nanostrength on the frequency sensitivity of the laminate composites, dynamic modulus and relaxation temperatures were measured by a Netzch DMA 242C dynamic mechanical analyser (DMA). The thermograms were obtained in torsional mode at vibration frequencies of 0.1, 1 and 10 Hz with a constant static load of 0.5 N and temperature ranging from 30 °C to 150 °C with a heating rate of 5 °C/min in air atmosphere. The specimens used for DMA analyses had dimensions of 25 × 12 × 1 mm^3.

3. Low velocity impact tests (drop tower)

For impact tests, specimens were cut from the composite plates at a size of 100*100 mm^2. Impact tests were carried out with a drop weight tower. This device consists of two columns attached to a metallic gantry (Fig. 2). These two columns guide the falling carriage, onto which different impactor geometries can be fixed. A winch with an electromagnet was used to lift the projectile (from 1 kg to 20 kg) to the desired impact height, function of the velocity required. During the test the projectile is released by an electromagnet, falls freely, and strikes the structure. An anti-bouncing
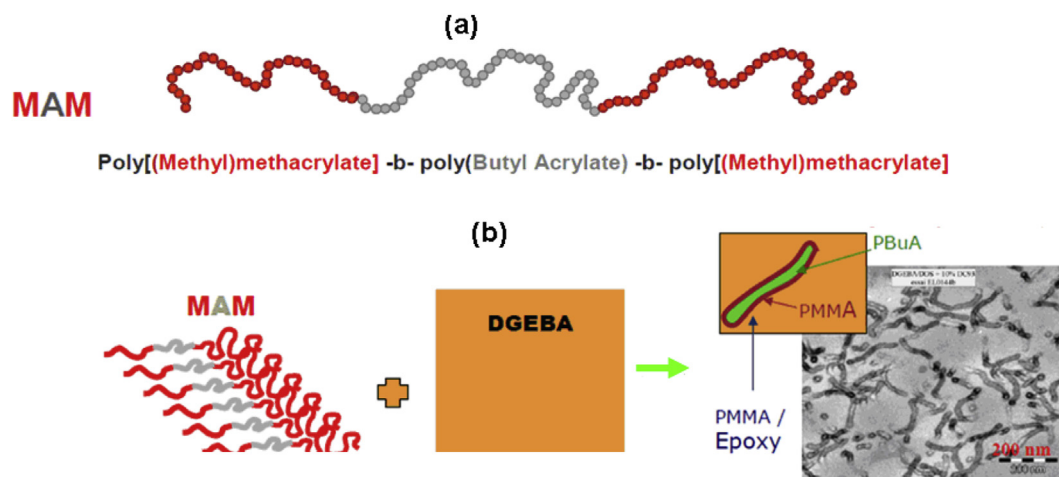
Fig. 1. (a) Schematic representation of Arkema's MAM Nanostrength® block copolymers, (b) TEM images of self assembled nanostructures in epoxy resin.

device is used to avoid a second shock, which could further damage the structure and prevent post-mortem analysis of the damage and residual strain. By placing a piezoelectric force sensor (Bruel&Kjaer 8230 C-003 force transducer, force range of 5 kN) under the projectile, the force response of the structure during impact can be recorded. During the test, the specimen was held under clamped edge conditions in a circular support 70-mm in diameter. The plates were clamped by four screws with a torque of 20 Nm. The steel impactor used for the study was a hemispherical impactor with 16-mm diameter. The impact tests were carried out at impact energies of 5.7 J, 9.6 J and 13.4 J, which corresponds to an impact velocity of 2.4, 3.1 and 3.7 ms^{-1} respectively, with a mass (carriage and impactor) equals to 1.95 kg. As a supplemental tool, a Photron FASTCAMAPX RS high-speed video camera was used to observe the lower face of the composite structure during the shock (a mirror was placed at 45° beneath the sample to reflect the image of the deformed sample; Fig. 2b). Displacement was measured through a second high-speed video camera (Photron SA3) that tracked a grid stuck on the impactor. For each type of composite the tests were repeated five times before validation, to ensure test repeatability.

4. Results and discussion

4.1. Materials morphology

Fig. 3 a and b shows topographic and phase AFM images of EPONS_FV. The relief is mainly due to the effect of the surface preparation, which is caused by the sputtering rate being different for the fibres and the matrix. The direction of the ion sputtering can also be identified by the shape of the surface corrugations. The AFM successfully confirms the presence of acrylic tri-block copolymers in the matrix. In topographic and phase images the Nanostrength is clearly identified. Nanostrength is present in the form of elongated micelles with dimensions of around one hundred nanometres. The spatial distribution of the micelles, which is clearly not affected by the ionic sputtering process, is very good -without the effect of clustering. These observations show that the matrix nano-structuration is as effective after woven fabrics impregnation as it is for the matrix in bulk system. This good dispersion of Nanostrength in EPONS_FV composite can be attributed to the ability of powdered Nanostrength to dissolve easily in the epoxy resin and to
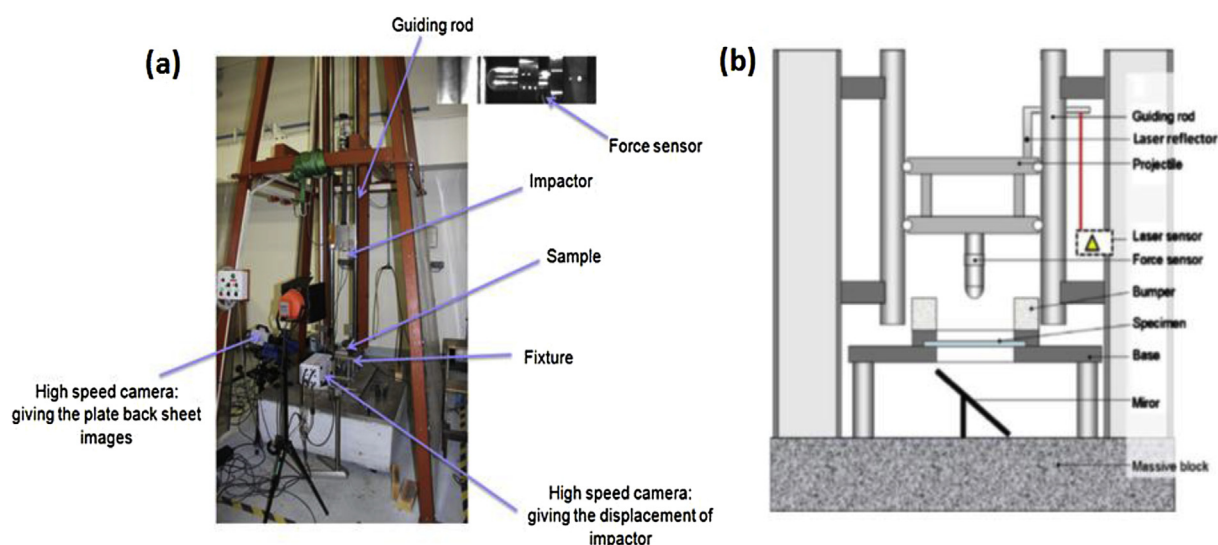

Fig. 2. Experimental set-up for low velocity impact tests: (a) Drop tower device; (b) Schematic representation of drop tower.
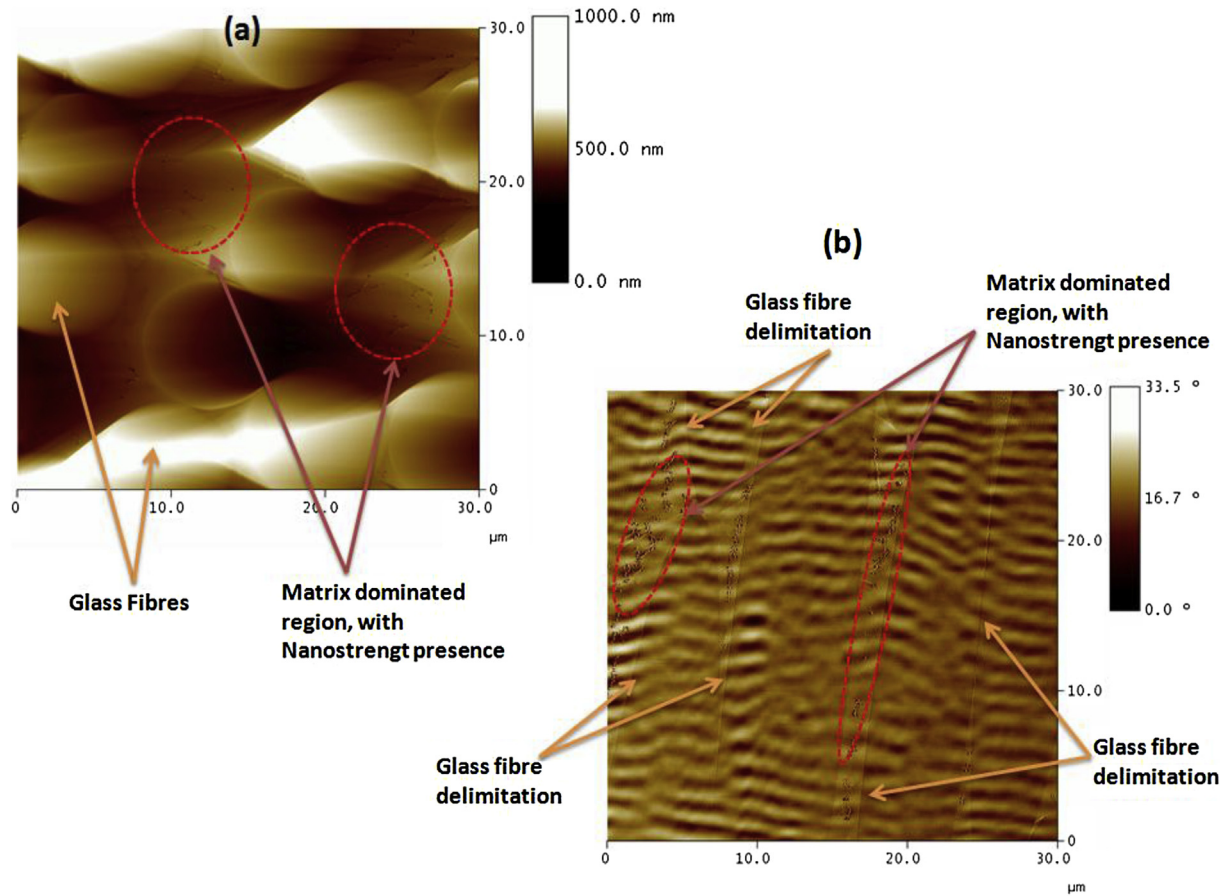
Fig. 3. AFM observations of EPONS_FV showing the presence of Nanostrength in form of elongated micelles: (a) topographic profile; (b) phase image of transverse fibres.

the role of the reactive diluent [30]. Working with neat epoxy, filled with Nanostrength, Arkema researchers showed that the best toughness improvement in pure epoxy was obtained when the Nanostrength was present as elongated micelles [31].

4.2. DMA and impact test results

The storage modulus G′, the loss modulus G″ and the variation of damping factor tan(delta) of EPO_FV and EPONS_FV are shown in

Fig. 4 a–b respectively. According to these results, the addition of Nanostrength leads to a decrease of the storage modulus, loss modulus and glass transition temperature(corresponding to the maximum of tan(delta)) (see Tables 1 and 2). This decrease is associated to the presence of both reactive diluent and nano-structured rubber phase [30]. As frequency increases, G′, G″ and Tg increase, showing a frequency/strain rate dependence of both materials [32]. However EPONS_FV displays the highest frequency/strain rate sensitivity. In fact, for EPO_FV, G′ increases only of about
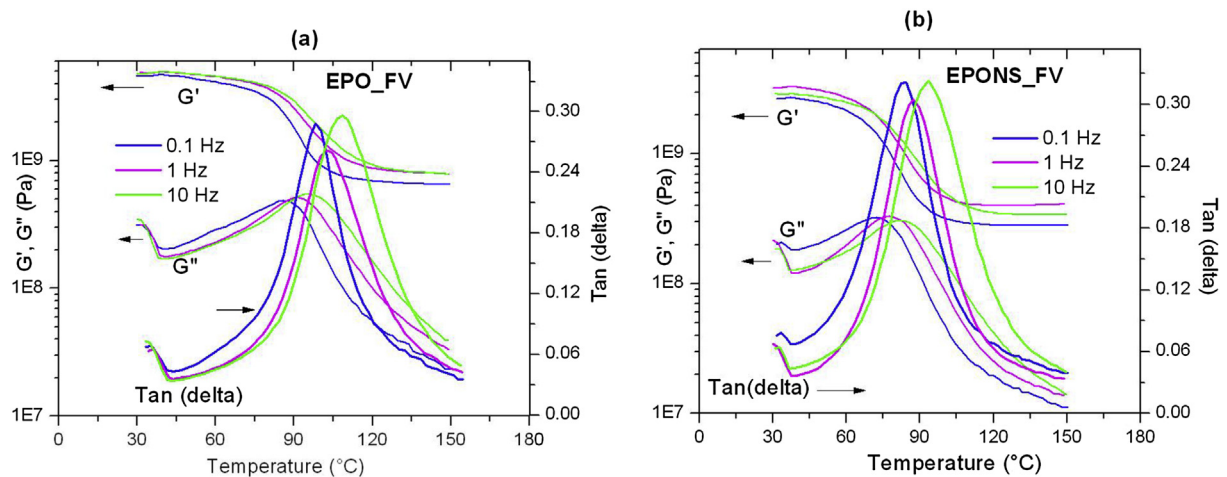

Fig. 4. Dynamic mechanical analysis (DMA) curves of (a) EPO_FV and (b) EPONS_FV for different frequencies.

Table 1
DMA values taken at a temperature of 40 °C for different frequencies.

	0.1 Hz		1 Hz		10 Hz	
Sample	G'(MPa)	G''(MPa)	G'(MPa)	G''(MPa)	G'(MPa)	G''(MPa)
EPO_FV	4700 ± 89	202.2 ± 6	4910 ± 73	176 ± 8	4940 ± 85	171 ± 5
EPONS_FV	2600 ± 56	190 ± 5	3250 ± 63	122 ± 4	2840 ± 45	132 ± 8

Table 2
Glass transition temperatures and activation energies of both EPO_FV and EPONS_FV.

Sample	T_g [°C, 0.1 Hz]	T_g [°C, 1 Hz]	T_g [°C, 10 Hz]	Activation energy [kJ mol^{-1}]
EPO_FV	94 ± 1.3	98 ± 1.2	104 ± 1.6	522.7 ± 3.8
EPONS_FV	84 ± 1.4	87 ± 1.5	93 ± 1.3	536.4 ± 3.2

4% when the frequency increases from 0.1 Hz to 1 Hz. While for EPONS_FV, G' increases of about 25% when the frequency increases from 0.1 Hz to 1 Hz. When the frequency increases from 0.1 Hz to 1 Hz, G'' decreases of about 12% and 35.7% for EPO_FV and EPONS_FV respectively.

To quantify the effect of Nanostrength on the epoxy chain mobility, the activation energy was calculated using the Arrhenius equation:

$$Ln\,f = Ln\,A - \frac{E_a}{RT_g}$$

where f is the frequency, A is a constant, R is the gas constant and T_g the glass transition temperature (in Kelvin) at a frequency of f. The activation energy was calculated from the slope of the natural logarithm of frequency versus the inverse of the glass transition temperature (T_g). From data reported in Table 2, it can be observed that the activation energy of EPONS_FV increases slightly with Nanotrength addition, showing that the epoxy chain's mobility is only slightly changed with the addition of Nanostrength.

Experimental results for EPO_FV specimens at an impact energy of 5.7 J are plotted in Fig. 5. Experimental data can be observed to be

quite repeatable (Fig. 5)(a) and in the following graphs, only one of these graphs is considered.

Typical force versus time curve, obtained during impact testing, is shown in Fig. 5(b). Time t0 and t4 correspond to the beginning and the end of the test. The total duration of the test is approximatively 10 ms. The curve was composed of four phases. The first phase (between [t0, t1]) corresponds to elastic bending of the composite plate. Between [t1, t2] the increase in load is less pronounced, revealing the first decrease of composite plate stiffness due to damage initiation. The damage consists mainly of matrix cracking, as illustrated by the presence of small oscillations in the plot [29]. The maximum force is reached at t2. Within the interval [t2, t3] the significant drop of load is due to damage propagation in the composite plate structure. The failure of fibres occurs in that stage. The last phase [t3, t4] corresponds to the residual strength of the composite plate and to dry friction during impactor penetration. The load at which damage initiation occurs is designated as F_{init}, the maximum load by F_{max}, the displacement corresponding to the maximum load by D_{Fmax}. Change in F_{init}, F_{max} and D_{Fmax} is the first method used to characterise the impact resistance of the composite plates.

Fig. 6 shows the load versus displacement response for both EPO_FV and EPONS_FV subjected to various levels of impact energies. The first part of the curves is very similar regardless of the composite, indicating that the Nanostrength addition does not affect the elastic behaviour of the structure. For both EPO_FV and EPONS_FV laminate composites, the increase of the peak force (F_{max}) with the impact energy is observed. These results agree with those of literature. From Fig. 6, it can be also observed that the effect of Nanostrength addition on the impact resistance clearly depends on the impact energy level. At 5.7 J, no improvement of impact resistance was observed; the maximum load remains approximately the same for EPO_FV and EPONS_FV. However, at 9.6 J and 13.4 J a significant improvement can be seen. For an impact energy of 9.6 J, this improvement consists of an enhancement of 28% in terms of F_{init}, 20% in terms of F_{max}, and 13.7% in terms of displacement corresponding to the maximum load. In fact, both F_{init} and F_{max} increase from 1195 N to 1390 N−1530 N and 1665 N with the addition of 10 wt% of Nanostrength. For an impact energy of 13.4 J, improvement can be estimated at around 20, 12.6 and
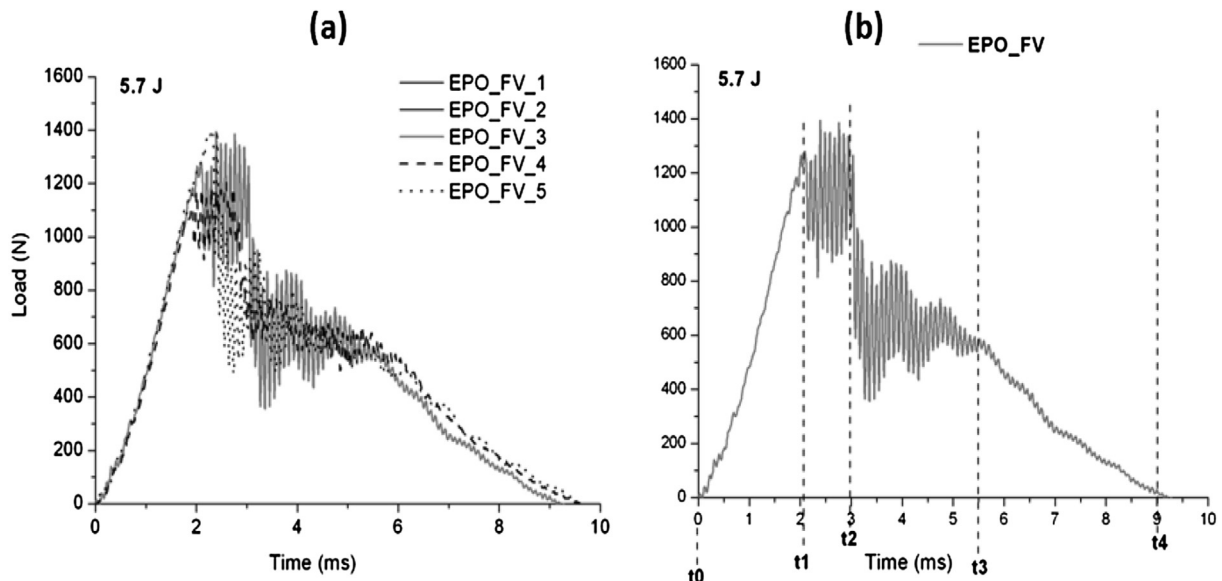

Fig. 5. Typical load vs time response at 5.7 J, showing tests repeatability.
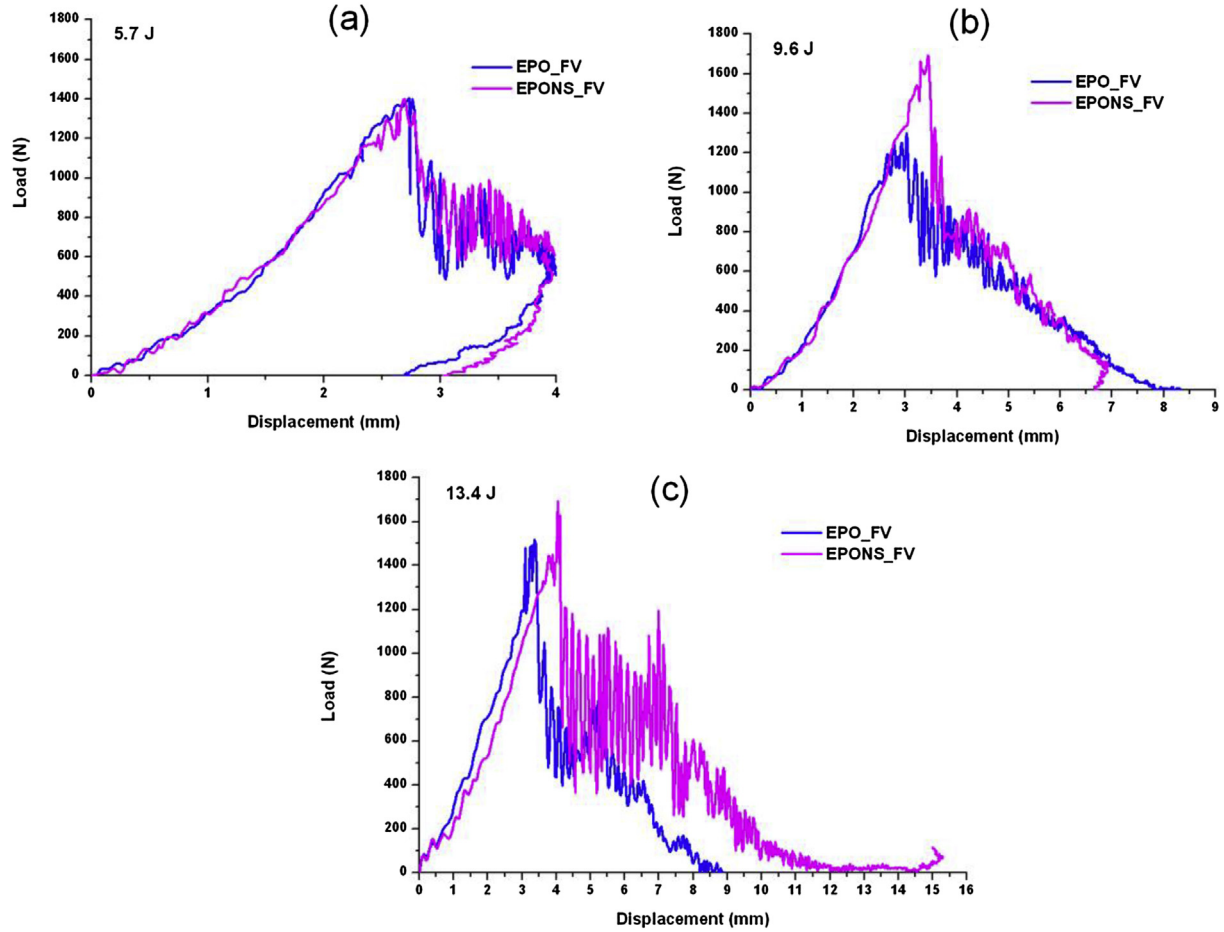
Fig. 6. Load versus displacement curves of EPO_FV and EPONS_FV subjected to different levels of impact energies.

16.6% for respectively F_{init}, F_{max} and the displacement. These values correspond to an increase from 1305 N to 1565N to 1505 N and 1695 N for F_{init} and F_{max} with addition of 10 wt% of Nanostrength.

Fig. 7 a–b shows the energy versus time curves of composites with neat epoxy and epoxy filled by Nanostrength. As seen from Fig. 7, each curve increases (during loading) with time, reaches a maximum value and then decreases (during unloading), and finally remains horizontal, reaching a constant value. This constant value gives the total energy absorbed by composite specimens at the end of an impact event. The maximum value of each curve represents the associated impact energies. The difference between them is termed as excessive energy (elastic energy), retained in the impactor and used to rebound the impactor from the non-perforated samples. From Fig. 7 it can be seen that in all cases at impact energy of 5.7 J, the absorbed energy in samples is slightly lower than the corresponding impact energy. The excessive impact energy is termed as elastic energy and is used for the impactor to rebound. At 9.6 J, the absorbed energy of laminate EPO_FV is equals to impact energy, showing that the penetration occurs for EPO_FV at this impact energy. For the same impact energy, laminate composite EPONS_FV presents a slight elastic energy, estimated at 0.6 J, showing that penetration does not take place. Therefore at 13.4 J the absorbed energy was found to be lower than impact energy for both composites. At this impact energy the two composite samples have been completely perforated. Obviously the elastic energy (Table 3) increases with the addition of Nanostrength for impact energies of 9.6 J. Impact results are listed in Table 3, including: F_{init}, F_{max}, displacement at maximum load, absorbed and elastic energies for all the laminate composites.

The penetration threshold is one the most important impact properties of composite laminates. This parameter can be used to determine the energy required to perforate the composite laminate. Many authors define different criteria to evaluate the penetration threshold. In our present work we used the criteria defined by Reis et al. [25] and Aktas et al. [33]. The authors defined an energy profile diagram (EPD). The diagram is useful for comparing the impact and absorbed energies, and for identifying the penetration and perforation thresholds. According to Aktas et al. [33], the penetration threshold can be defined as the point where the absorbed energy equals the impact energy.

Fig. 8 shows the energy profile diagram (EPD) of EPO_FV and EPONS_FV at ambient temperature. The diagram shows that when the impact energy is between 5.7 and 9.6 J, data points of EPONS_FV are found to be below the equal energy line, meaning that the penetration threshold was not reached in this region and therefore excessive energy is consumed to rebound the impactor. At 9.6 J the absorbed energy of EPO_FV is found to be equals to impact energy, showing that the penetration has occurred. By increasing level of impact energy (13.4 J), the data points of both laminates lie below the equal energy line, showing that the composites are completely perforated. This last observation allows us to conclude that the penetration threshold of EPONS_FV is situated between 9.6 J and 13.4 J.

Fig. 9 shows data points of elastic energy (Ee) versus impact energy (Ei) and corresponding polynomial fitting. The elastic energy was calculated as the difference between the absorbed impact energy and the energy at the peak load [25]. The roots of the polynomial equations give energy points where impact energy (Ei)
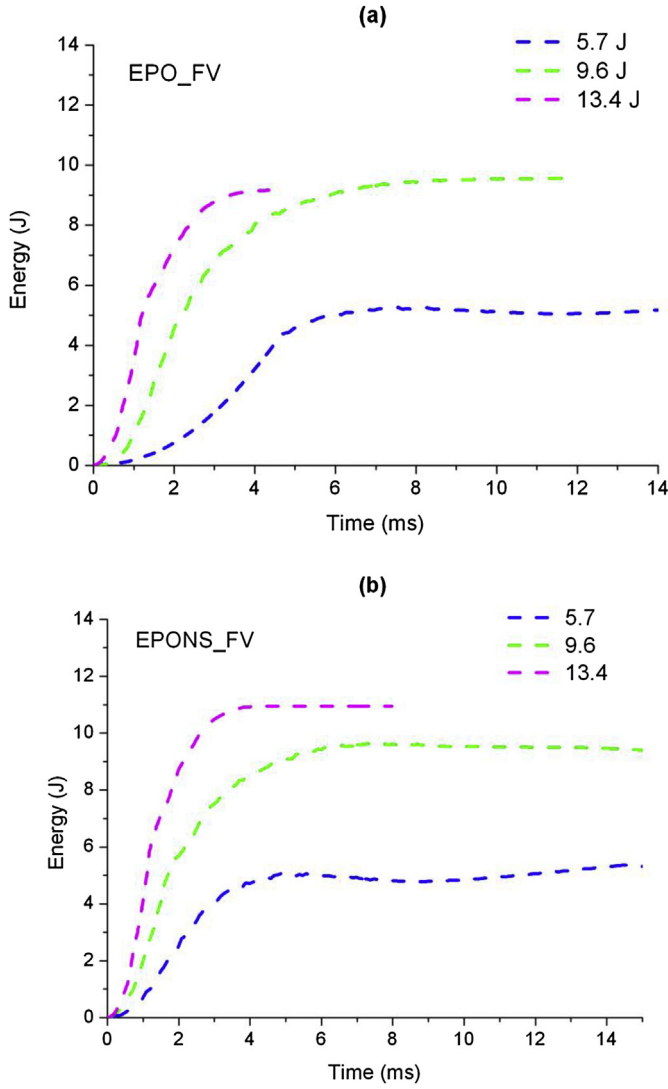
Fig. 7. Energy versus time diagrams for composites: (a) with neat epoxy, (b) with epoxy filled by Nanostrength.
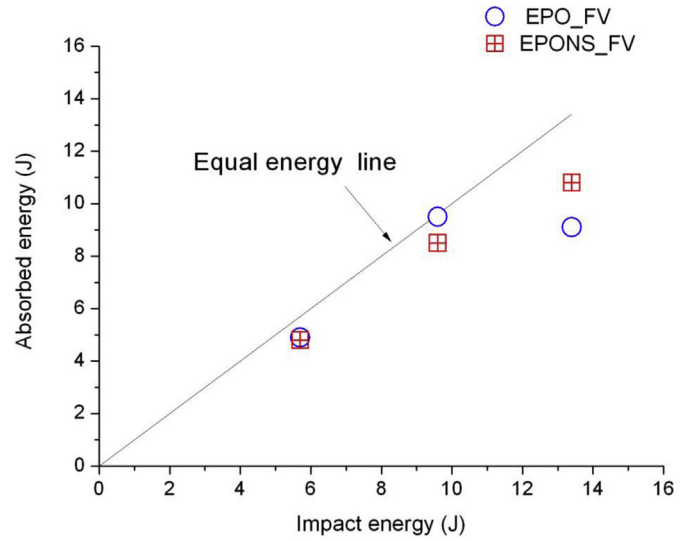

Fig. 8. The energy profile diagram (EPD).

different approaches are used. These approaches consist of using comptabilizing agents, toughening the interface regions between plies or toughening the epoxy matrix. In our case, the method used consists of toughening the epoxy matrix. Thus, the mechanism leading to the improvement of the impact resistance is mainly due to epoxy modification and its effect on both matrix toughness and the quality of interfacial adhesion between the modified matrix and the glass fibres. The toughness improvement of epoxy, through the formation of a nanostructured phase, could be related to the fact that the elastomeric phase (PBu) is homogenously dispersed in the epoxy matrix at a nanometre scale(see AFM section), which could greatly enhance the interaction between the epoxy matrix and Nanostrength. Since Nanostrength is reactive, some chemical bonds between the epoxy matrix and Nanostrength can be created. Some authors [34,35]reported that any mechanism that facilitates the shear localization process, or alternatively dissipates the bulk strain energy, would enhance the toughness. The rubber nanophase in acrylic tri-block copolymer appears to do both. According to the works of Pearson et al [35,36], at a sufficiently high strain rate, when the neat epoxy dilates at a nearly constant rate, the rubber
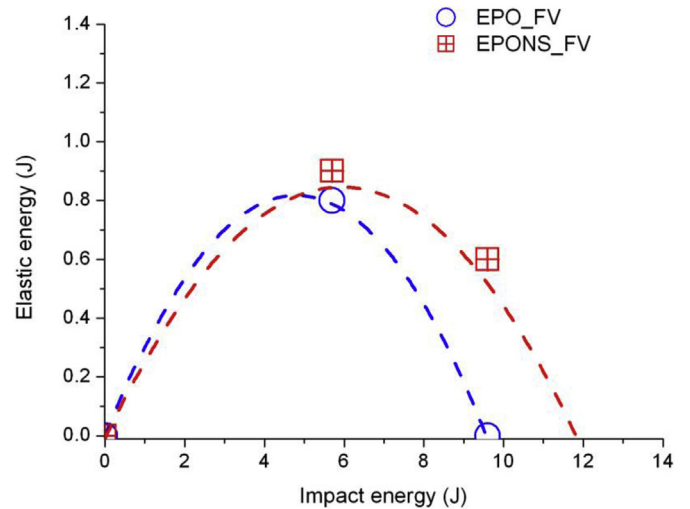
is equal to absorbed energy (Ea), i.e. where Ee = 0. The higher roots imply penetration thresholds for both laminates [25,33]. They are 9.6 J and 11.8 J for EPO_FV and EPONS_FV respectively. Thus, the difference between them is 2.2 J. This difference is small. The main reason for this: the polynomial fitting was only done for three points. However, the addition of Nanostrength increases the penetration threshold.

Concerning the mechanisms leading to an improvement of the impact resistance, different ideas can be advanced. Conventionally, to improve the toughness of fibre eboxy laminate composites, three

Table 3
Impact test results.

	F_{init} (N)	F_{max} (N)	Displacement D_{Fmax} (mm)	Absorbed energy (J)	Elastic energy (J)
EPO_FV (5.7J)	1050 ± 36	1385 ± 49	2.8 ± 0.5	4.9 ± 0.4	0.8 ± 0.05
EPONS_FV (5.7 J)	1190 ± 33	1387 ± 51	2.7 ± 0.4	4.8 ± 0.4	0.9 ± 0.1
EPO_FV (9.6 J)	1195 ± 30	1390 ± 43	2.9 ± 0.6	9.5 ± 0.2	0
EPONS_FV (9.6 J)	1530 ± 37	1665 ± 45	3.3 ± 0.8	8.6 ± 0.3	0.6 ± 0.05
EPO_FV (13.4 J)	1305 ± 29	1505 ± 37	3.6 ± 0.6	9.1 ± 0.3	−
EPONS_FV (13.4 J)	1565 ± 33	1695 ± 40	4.2 ± 0.5	10.9 ± 0.2	−

Fig. 9. Identification of penetration threshold.

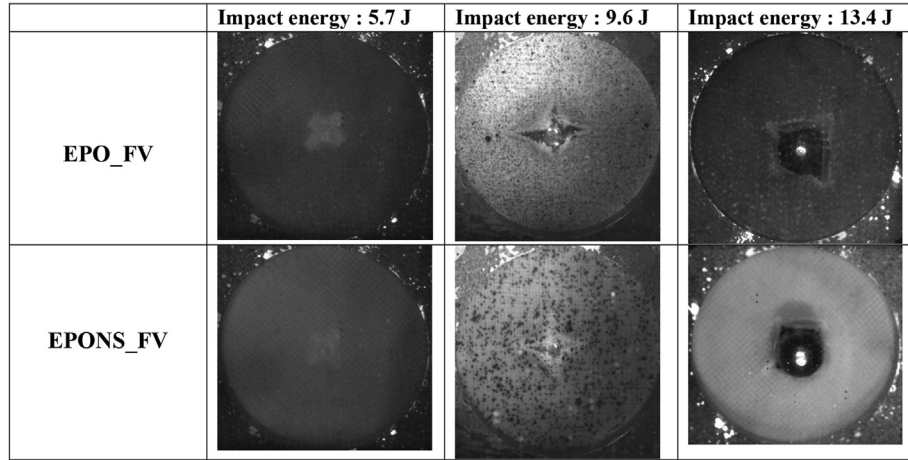|	Impact energy : 5.7 J	Impact energy : 9.6 J	Impact energy : 13.4 J
EPO_FV			
EPONS_FV			

Fig. 10. Pictures of bottom surface of both EPO_FV and EPONS_FV plates after impact.

particles cause the material to expand at a higher rate than neat epoxy. They conclude that this expansion was induced by cavitation of the rubber particles. Thus, we assume that the rubber particles facilities the sample expansion by cavitation.

4.3. Damage quantification

Fig. 10 presents pictures of impacted plates with both EPO_FV and EPONS_FV, for different impact energies. When plates with Nanostrength are compared to those without Nanostrength, at a given impact energy, the general trend is that the damage size is much lower in plates with Nanostrength. The four-sided pyramidal fracture is attributed to the use of the bi-directional woven fabric composite plates. Typical micrographs taken on impacted sample section of both EPO_FV and EPONS_FV are shown in Figs. 11 and 12. The major damage modes of the two composite plates are delamination, fibre breakage at the back surface and matrix cracking. This observation agrees with another report on hybrid laminate composites [37]. Fibre breakage occurs on the centrally depressed zone for both composites. As reported in other works, fibre breakage is

due to locally high stresses and indentation effects [38,39]. For both composites delamination mainly developed at 0/90° interfaces, this was due to the different flexural stiffness of adjacent layers [38]. According to the optical observations, EPO_FV seems to present a larger delamination zone compared to that of EPONS_FV. However, matrix cracks, in form of shear failure mode, propagated radially from the top down, inclined at about ±45° from the vertical position, for the two composites. As for delamination, the matrix cracking is more visible in EPO_FV than in EPONS_FV, indicating that the addition of Nanostrength in the epoxy matrix contributes to preventing both delamination and matrix cracking. This observation agrees with the work of Denneulin et al. [29], where the authors demonstrated that the addition of Nanostrength in the epoxy matrix allows the epoxy matrix to be more ductile. In ductile materials, damage takes place mainly by cavitation. This fact could explain why matrix cracking and delamination are less developed in the case of EPONS_FV.

Scanning electron microscopy (SEM) (JSM 840 device) was used to investigate the composite plates after impact testing. SEM analysis was conducted on ion polished plates to examine the
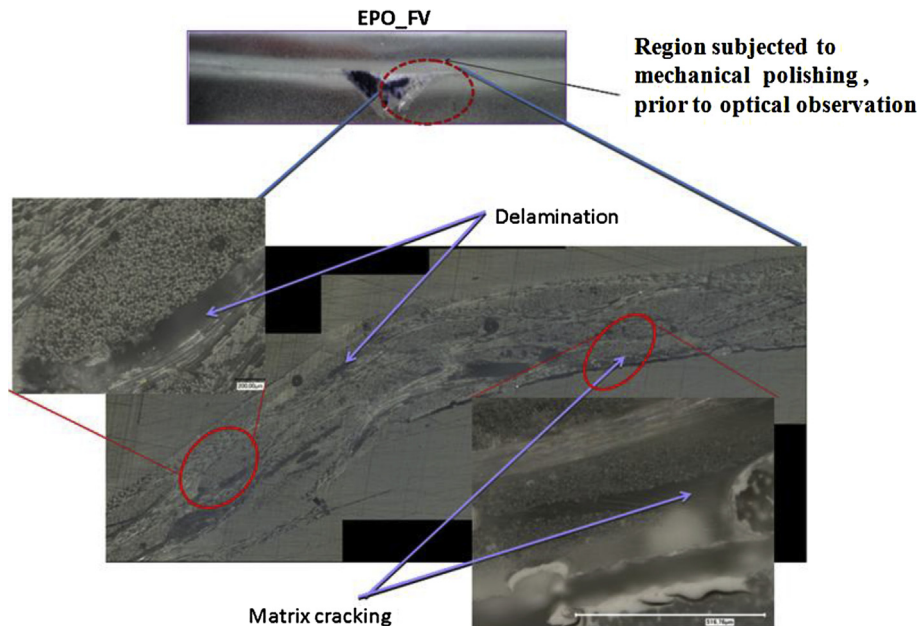

Fig. 11. Optical observation of the section of EPO_FV (9.6 J impact) after impact.
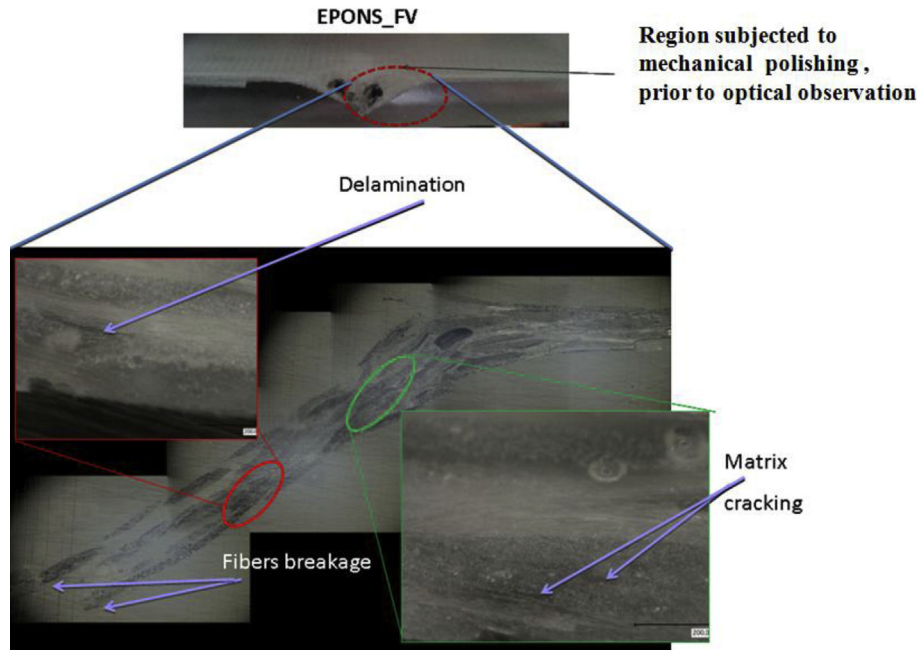
Fig. 12. Optical observation of the section of EPONS_FV (9.6 J impact) after impact.

fracture surface of EPO_FV and EPONS_FV and to observe the micro-cracks in the matrix. In the case of composites without Nanostrength (EPO_FV), cracks propagate in a longitudinal direction (see Fig. 13), whereas with Nanostrength (EPONS_FV) they propagate in a transverse direction (see Fig. 14). Both composite micro-cracks consist of coalescence of fibre matrix decohesion. It appears that the micro-crack density changes with the addition of Nanostrength in epoxy resin. The composites with Nanostrength seem to have lower micro-cracks density compared to those without Nanostrength. In addition, the size of micro-cracks for the EPONS_FV seems smaller than that of the EPO_FV laminate composite (this argument remains qualitative one).

Impact results and damage observations show a beneficial effect of Nanostrength addition, particularly for a high impact energy level. The viscoelastic behaviour of both materials provides information on the mechanical and strain rate sensitivity. This can therefore explain why the effect of Nanostrength addition appears at high energy. Indeed, DMA analyses showed that EPONS_FV
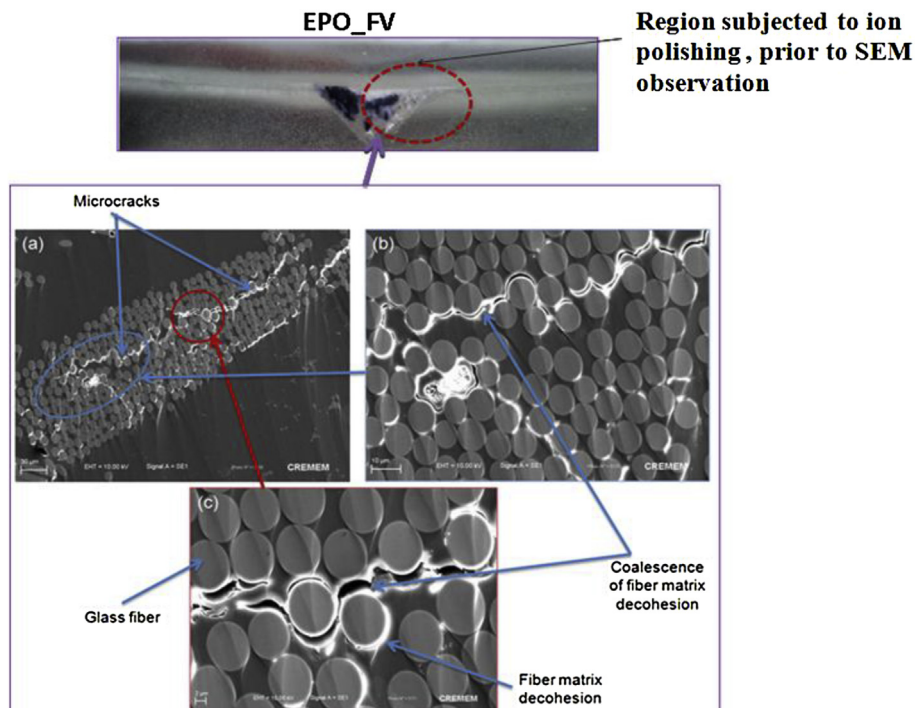

Fig. 13. SEM images of EPO_FV_10 ion polishing plate at different magnifications. (9.6 J impact) after impact.
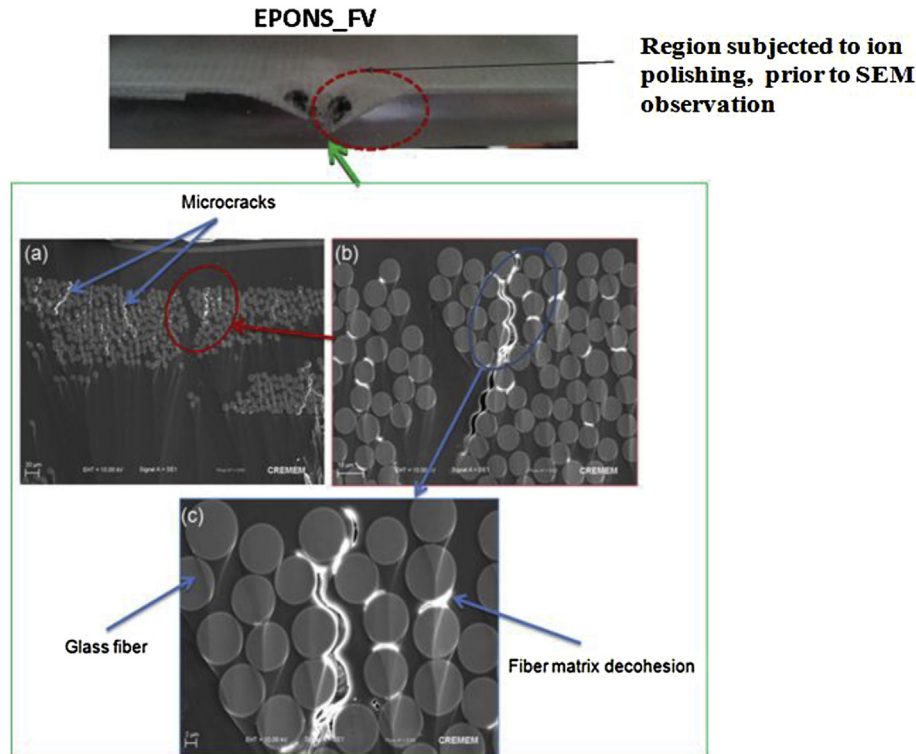
Fig. 14. SEM images of impacted EPONS_FV_10 ion polishing plate at different magnifications(9.6 J impact).

displays the highest frequency/strain rate sensitivity compared to EPO_FV. From a material point of view, this effective strain rate sensitivity of EPONS_FV could explain why the increased toughness appears at a high impact energy level. This fact is confirmed from the evaluation of the activation energy, showing that the epoxy chain's mobility is only slightly changed with the addition of Nanostrength. This information leads us to conclude that adding acrylic tri-block copolymer leads to an improvement of the impact resistance without affecting the epoxy polymer chains mobility.

Damage investigation showed that Nanostrength addition can improve the micro-crack resistance of composites. Ahead of the crack front, Nanostrength seems to be able to interact within the plastic zone by suppressing coalescence of micro-cracks and voids [28]. The Nanostrength may act to shield the matrix from damage by crack bridging. The toughening of epoxy modified Nanostrength composites is also caused by the micelle cavitation [40,41], which can induce matrix shear banding [42]. This last argument seems to be the most predominant in the case of EPONS_FV, since the density of micro-cracks was found to be lower when Nanostrength was added into the epoxy matrix. Thus, the addition of Nanostrength into the epoxy matrix leads to sample elastic expansion by micelles cavitation. This results in a decrease of micro-cracks density. All these observation are in agreement with the impact resistance results, where an improvement was shown with addition of Nanostrength.

5. Conclusions

Composite laminates have been produced by using glass fibre fabrics and epoxy modified tri-block copolymers as a matrix. The effect of the introduction of these tri-block copolymers into the matrix has been investigated through analysis of the impact resistance properties. AFM results showed good dispersion of tri-block copolymers in the composite's matrix and DMA analyses characterised the effect of Nanostrength addition on the visco-elastic behaviour of the material. The effect of tri-block copolymer addition has been analysed through impact tests with low velocity impact. Results obtained for three impact energies showed that the impact resistance of the composite is affected by the presence of tri-block copolymers. This increase is more significant at high impact energy level. It also showed that the threshold penetration is slightly increased with the addition of tri-block copolymers. SEM observations performed on plates after impact tests showed that the main damage mechanisms in both composites are matrix cracking, delamination and fibre breakage. It was also shown that EPONS_FV depicted a lower micro-crack density than EPO_FV, showing that the toughening of epoxy-modified Nanostrength composites is caused by the micelle cavitation, which can induce matrix shear banding. The use of a tri-block copolymer in the epoxy matrix is a good method to overcome primary issues of rigid epoxy-fibre composites, i.e. the material cost and the impact properties, without compromising the others physical properties, such as glass transition temperature or elastic modulus. Our conclusions can be used in other fields, such as the automobile and naval industries.

Acknowledgements

References

[1] Amaro AM, Reis PNB, De Moura MFSF, Santos JB. Damage detection on laminated composite materials using several NDT techniques. Insight: Non-Destructive Test Cond Monit 2012;54(1):14—20.
[2] Adams RD, Cawley P. A review of defect types and nondestructive testing techniques for composites and bonded joints. NDT Int 1988;21(4):208—22.

[3] Argüelles A, Viña J, Canteli AF, Coronado P, Mollón V. Influence of temperature on the delamination process under mode I fracture and dynamic loading of two carbon–epoxy composites. Compos Part B: Eng 2015;68(0):207–14.

[4] Amaro AM, Reis PNB, Moura MFSF. Residual strength after low velocity impact in carbon-epoxy laminates. Mater Sci Forum 2006:624–8.

[5] Vejen N, Pyrz R. Transverse crack growth in glass/epoxy composites with exactly positioned long fibres. Part I: Exp Compos Part B: Eng 2001;32(7):557–64.

[6] Caprino G. Residual strength prediction of impacted cfrp laminates. J Compos Mater 1984;18(6):508–18.

[7] Prichard JC, Hogg PJ. The role of impact damage in post-impact compression testing. Composites 1990;21(6):503–11.

[8] Davies GAO, Hitchings D, Zhou G. Impact damage and residual strengths of woven fabric glass/polyester laminates. Compos Part A: Appl Sci Manuf 1996;27(12):1147–56.

[9] de Moura MFSF, Marques AT. Prediction of low velocity impact damage in carbon–epoxy laminates. Compos Part A: Appl Sci Manuf 2002;33(3):361–8.

[10] Amaro AM, Reis PNB, De Moura MFSF. Delamination effect on bending behaviour in carbon-epoxy composites. Strain 2011;47(2):203–8.

[11] Reis PNB, Ferreira JAM, Antunes FV, Richardson MOW. Effect of interlayer delamination on mechanical behavior of carbon/epoxy laminates. J Compos Mater 2009;43(22):2609–21.

[12] Lalande L, Plummer CJG, Månson JAE, Gérard P. Microdeformation mechanisms in rubber toughened PMMA and PMMA-based copolymers. Eng Fract Mech 2006;73(16):2413–26.

[13] Kanny K, Mohan TP. Resin infusion analysis of nanoclay filled glass fiber laminates. Composites Part B: Engineering. (0).

[14] Ireland R, Arronche L, La Saponara V. Electrochemical investigation of galvanic corrosion between aluminum 7075 and glass fiber/epoxy composites modified with carbon nanotubes. Compos Part B: Eng 2012;43(2):183–94.

[15] Kornmann X, Rees M, Thomann Y, Necola A, Barbezat M, Thomann R. Epoxy-layered silicate nanocomposites as matrix in glass fibre-reinforced composites. Compos Sci Technol 2005;65(14):2259–68.

[16] Manfredi LB, De Santis H, Vázquez A. Influence of the addition of montmorillonite to the matrix of unidirectional glass fibre/epoxy composites on their mechanical and water absorption properties. Compos Part A: Appl Sci Manuf 2008;39(11):1726–31.

[17] Matadi Boumbimba R, Bouquey M, Muller R, Jourdainne L, Triki B, Hébraud P, et al. Dispersion and morphology of polypropylene nanocomposites: characterization based on a compact and flexible optical sensor. Polym Test 2012;31(6):800–9.

[18] Matadi R, Gueguen O, Ahzi S, Gracio J, Muller R, Ruch D. Investigation of the stiffness and yield behaviour of melt-intercalated poly(methyl methacrylate)/organoclay nanocomposites: characterisation and modelling. J Nanosci Nanotechnol 2010;10(4):2956–61.

[19] Hourston DJ, Lane JM. The toughening of epoxy resins with thermoplastics: 1. trifunctional epoxy resin-polyetherimide blends. Polymer 1992;33(7):1379–83.

[20] Ashrafi B, Guan J, Mirjalili V, Zhang Y, Chun L, Hubert P, et al. Enhancement of mechanical performance of epoxy/carbon fiber laminate composites using single-walled carbon nanotubes. Compos Sci Technol 2011;71(13):1569–78.

[21] Gojny FH, Wichmann MHG, Fiedler B, Bauhofer W, Schulte K. Influence of nano-modification on the mechanical and electrical properties of conventional fibre-reinforced composites. Compos Part A: Appl Sci Manuf 2005;36(11):1525–35.

[22] Hosur MV, Mohammed AA, Zainuddin S, Jeelani S. Processing of nanoclay filled sandwich composites and their response to low-velocity impact loading. Compos Struct 2008;82(1):101–16.

[23] Ávila AF, Carvalho MGR, Dias EC, da Cruz DTL. Nano-structured sandwich composites response to low-velocity impact. Compos Struct 2010;92(3):745–51.

[24] Iqbal K, Khan S-U, Munir A, Kim J-K. Impact damage resistance of CFRP with nanoclay-filled epoxy matrix. Compos Sci Technol 2009;69(11–12):1949–57.

[25] Reis PNB, Ferreira JAM, Zhang ZY, Benameur T, Richardson MOW. Impact response of Kevlar composites with nanoclay enhanced epoxy matrix. Compos Part B: Eng 2013;46(0):7–14.

[26] Reis PNB, Ferreira JAM, Zhang ZY, Benameur T, Richardson MOW. Impact strength of composites with nano-enhanced resin after fire exposure. Compos Part B: Eng 2014;56(0):290–5.

[27] Arkema launches nanostrength for advanced composite materials. Addit Polym 2005;2005(6):3.

[28] Bashar MT, Sundararaj U, Mertiny P. Mode-I interlaminar fracture behaviour of nanoparticle modified epoxy/basalt fibre-reinforced laminates. Polym Test 2013;32(2):402–12.

[29] Denneulin S, Viot P, Leonardi F, Lataillade J-L. The influence of acrylate triblock copolymer embedded in matrix on composite structures' responses to low-velocity impacts. Compos Struct 2012;94(4):1471–81.

[30] Matadi Boumbimba R, Froustey C, Viot P, Olive JM, Léonardi F, Gerard P, et al. Preparation and mechanical characterisation of laminate composites made of glass fibre/epoxy resin filled with tri bloc copolymers. Compos Struct 2014;116(0):414–22.

[31] Tran TA, Leonardi F, Bourrigaud S, Gerard P, Derail C. All acrylic block copolymers based on poly (methyl methacrylate) and poly (butyl acrylate). A link between the physico-chemical properties and the mechanical behaviour on impact tests. Polym Test 2008;27(8):945–50.

[32] Wang K, Ahzi S, Matadi Boumbimba R, Bahlouli N, Addiego F, Rémond Y. Micromechanical modeling of the elastic behavior of polypropylene based organoclay nanocomposites under a wide range of temperatures and strain rates/frequencies. Mech Mater 2013;64(0):56–68.

[33] Aktaş M, Atas C, İçten BM, Karakuzu R. An experimental investigation of the impact response of composite laminates. Compos Struct 2009;87(4):307–13.

[34] Liang YL, Pearson RA. The toughening mechanism in hybrid epoxy-silica-rubber nanocomposites (HESRNs). Polymer 2010;51(21):4880–90.

[35] Pearson RA, Bacigalupo LN. Epoxies toughened with self-assembling block copolymers. In: ACS 241st National Meeting; Anaheim, CA; 2011. URL accessed on 7/29/2013 at, http://www.adhesionsociety.org/wp-content/uploads/2013-Annual-Meeting-Abstracts/Chen_Epoxies_2013.pdf.

[36] Pearson RA, Yee AF. Toughening mechanisms in elastomer-modified epoxies – part 3: the effect of cross-link density. J Mater Sci 1989;24(7):2571–80.

[37] Sarasini F, Tirillò J, Ferrante L, Valente M, Valente T, Lampani L, et al. Drop-weight impact behaviour of woven hybrid basalt–carbon/epoxy composites. Compos Part B: Eng 2014;59(0):204–20.

[38] Shyr T-W, Pan Y-H. Impact resistance and damage characteristics of composite laminates. Compos Struct 2003;62(2):193–203.

[39] Cantwell WJ, Morton J. Comparison of the low and high velocity impact response of cfrp. Composites 1989;20(6):545–51.

[40] Wu J, Thio YS, Bates FS. Structure and properties of PBO–PEO diblock copolymer modified epoxy. J Polym Sci Part B: Polym Phys 2005;43(15):1950–65.

[41] Yang X, Yi F, Xin Z, Zheng S. Morphology and mechanical properties of nanostructured blends of epoxy resin with poly(ε-caprolactone)-block-poly(butadiene-co-acrylonitrile)-block-poly(ε-caprolactone) triblock copolymer. Polymer 2009;50(16):4089–100.

[42] Bashar M, Sundararaj U, Mertiny P. Study of matrix micro-cracking in nano clay and acrylic tri-block-copolymer modified epoxy/basalt fiber-reinforced pressure-retaining structures. Express Polym Lett 2011;5(10):882–96.